

# Vertical Uplift Capacity of Circular Anchor Plates

P. Bhattacharya<sup>1</sup> and J. Kumar<sup>2</sup>

<sup>1</sup>Department of Civil Engineering, Indian Institute of Technology, Kharagpur, India

<sup>2</sup>Department of Civil Engineering, Indian Institute of Science, Bangalore, India

E-mails: paramita@civil.iitkgp.ernet.in, jkumar@civil.iisc.ernet.in

**ABSTRACT:** Experimental and numerical investigations have been carried out to determine the vertical uplift resistance of circular anchor plates embedded in cohesionless soil media. Experimental studies are performed on model circular anchor plates placed at different depths in loose to medium dry sand deposit for two different relative densities, namely, 25% and 65%, respectively. The numerical work has been done by using an axisymmetric lower bound limit analysis in conjunction with finite elements and linear programming to compute the uplift resistance offered by circular anchor plates embedded horizontally in sand. In the case of numerical studies, the internal frictional angle of sand was varied from 20° to 45°. Both experimental and numerical studies clearly reveal that the uplift resistance of the circular plate increases considerably with increases in embedment ratio ( $H/D$ ), and soil frictional angle( $\phi$ ). The deformation of the anchor plate, corresponding to the failure load, increases with an increase in the values of  $H/D$  and relative density of sand. The values of the failure loads obtained from the computational analysis match well with the present experimental results as well with the available data from literature.

**Keywords:** Circular anchors, failure, load deformation response, limit analysis, sand.

## 1. INTRODUCTION

Horizontal anchor plates are often employed to resist the uplift forces. Foundations of transmission towers, utility poles, aircraft moorings, submerged pipelines are a few typical examples where horizontal anchors are used to generate the uplift resistance. Many research investigations in the past were reported based on (i) 1-g small scale laboratory model tests (Das and Seeley 1975), (ii) the limit equilibrium method (Meyerhof 1973), (iii) the displacement based elasto-plastic finite element method (Rowe and Davis 1982), (iv) the upper bound limit analysis (Kumar 2001, Merifield et al. 2006, Merifield and Sloan 2006 and Kumar and Kouzer 2008), and (v) the lower bound limit analysis (Merifield and Sloan 2006). These investigations are mainly meant for strip anchor plates. A few experimental investigations have also been reported on horizontal anchor plates with the shapes other than the strip anchor (Balla 1961, Sutherland 1965, Baker and Konder 1966, Ilamparuthi et al. 2002). By applying Kotter's equation, Balla (1961) proposed a simplified theoretical analysis based on laboratory investigations for mushroom foundations of pylons. A circular failure surface was assumed by Balla (1961). Several small scale model tests were carried out by Baker and Konder (1966) on earth anchors and their results were found to agree generally well with the earlier data reported by Balla (1961) for anchors with embedment depth below  $6D$ ; where  $D$  is the diameter of the anchor plate. Sutherland (1965) indicated that the mode of failure for anchors in sand depends mainly upon the relative density of sand. Murray and Geddes (1987) performed both experimental and theoretical investigations for finding out the uplift capacity of circular anchor plates embedded in medium to dense sands. The lower bound solution obtained by Murray and Geddes (1987) was, however, not found to be very satisfactory. The upper bound solution provided by Murray and Geddes (1987) overestimated the pullout load as compared to the experimental results. Merifield et al. (2006) have determined the uplift capacity of circular anchor plates by performing a three dimensional lower bound limit analysis. The current research work examines in a detailed fashion the pullout capacity of circular anchor plates by performing (i) the numerical axisymmetric lower bound limit analysis, and (ii) a series of small laboratory tests for anchors buried in sand. The uplift resistance has been determined for different embedment ratios and relative densities.

## 2. PROBLEM DEFINITION

A circular anchor having diameter equal to  $D$  is placed over homogeneous sand stratum. The thickness of this plate is assumed to be negligible as compared to its diameter, and  $H$  is the depth of the

top surface of the anchor plate measured from ground surface as shown in Figure 1; it is given that  $\delta$  is the friction angle between the interface of the anchor plate and surrounding soil mass. It is assumed that uniform surcharge pressure  $q$  acts over ground surface. It is required to determine the ultimate pullout load  $P_u$  per unit area ( $A$ ) of the circular anchor plate. The pullout capacity factors  $F_\gamma$  and  $F_q$  are defined by using the following equations:

$$F_\gamma = \frac{P_u}{A\gamma H} \quad \text{where } q = 0 \text{ and } \gamma \neq 0 \quad (1)$$

$$F_q = \frac{P_u}{Aq} \quad \text{where } q \neq 0 \text{ and } \gamma = 0 \quad (2)$$

## 3. EXPERIMENTAL MODELLING

All the experiments were conducted in a rectangular tank of size 1.8 m (length)  $\times$  0.9 m (width)  $\times$  0.8 m (height). The walls of the tank were made by 10 mm thick glass sheet. The sides and bottom of the tank were strengthened by providing vertical and horizontal stiffeners. The experiments were performed by using a circular steel anchor plate having 50 mm diameter and 8 mm thickness. Two dial gauges, with a displacement sensitivity of 0.01 mm, were placed normal to steel plate as shown in Figure 2(a) to measure the displacements of the anchor plate. The vertical displacements were taken as the average of the two dial gauges' readings. The loading frame consists of two vertical channel sections anchored into a concrete platform of size 1.5 m  $\times$  2.0 m. These channels were placed at a distance of 1.0 m and provided with adequate lateral support at the bottom. These vertical channels were further stiffened by two lateral channels at the top. Two pulley brackets were mounted to conduct the pullout test where one was mounted at the centre of the horizontal stiffeners and another one was at the end of horizontal stiffeners. The vertical uplift load was applied on the anchor plate by using a steel wire which moves freely over a coupling of two pulleys and connected with a gravity type loading arrangement. The loading arrangement was such that it pulls out the anchor plate vertically upward by placing the weights on its other end.

## 4. SAND PROPERTIES AND SAMPLE PREPARATION

The sand used for the present experimental investigation was prepared by mixing two different types of local sands so that 65% of the maximum density can be achieved. The relative density test was carried out as per Indian Standard Code (IS: 2720 Part 4 - 1985). The minimum and maximum mass densities of sand sample 1 were

found to be equal to  $\rho_{min} = 1.42 \text{ g/cc}$  and  $\rho_{max} = 1.64 \text{ g/cc}$ , respectively. On the other hand,  $\rho_{min} = 1.54 \text{ g/cc}$  and  $\rho_{max} = 1.82 \text{ g/cc}$  were noted for sand sample 2. The sand sample 3 (S3) was prepared by adding 70% of sample 1 and 30% of sample 2 in such a way that the minimum and maximum mass densities of the newly prepared sample become equal to  $\rho_{min} = 1.48 \text{ g/cc}$  and  $\rho_{max} = 1.71 \text{ g/cc}$ , respectively. Specific gravity, grain size distribution, mass density and direct shear tests were performed as per Indian Standard Code to characterize the sand sample. The specific gravity ( $G$ ) for the foundation material was found to be 2.64, and maximum and minimum void ratios are equal to  $e_{max} = 0.78$  and  $e_{min} = 0.54$ , respectively. The grain size distribution curve for the foundation material was plotted based on the sieve analysis and following parameters are quantified:  $D_{10} = 0.2 \text{ mm}$ ,  $D_{30} = 0.3 \text{ mm}$  and  $D_{60} = 0.6 \text{ mm}$ ,  $C_u = 3$  and  $C_c = 0.75$  where  $D_{10}$ ,  $D_{30}$ ,  $D_{60}$  are diameters corresponding to 10%, 30% and 60% finer, respectively, and  $C_u$  and  $C_c$  are coefficients of uniformity and curvature, respectively. It was concluded that the material chosen is a poorly graded sand. The direct shear test, confirming IS: 2720-1986 Part 13, was performed to find out the soil internal friction angle. By using direct shear test, for each mass density of soil, tests were conducted at four different values of the normal stresses. For a vertical normal stress range of 50 kPa to 150 kPa, the peak internal friction angles ( $\phi_p$ ) of the chosen sand were found to be  $29.6^\circ$  and  $37.8^\circ$  corresponding to  $\rho_d = 1.53 \text{ g/cc}$  and  $\rho_d = 1.62 \text{ g/cc}$ , respectively.

model anchors in the laboratory. It is a difficult task to measure the value of the peak friction angle in such a low stress range based on direct shear tests. For a low stress levels, varying from 2 kPa to 30 kPa, the peak friction angle of the chosen sand sample was indirectly determined at two relative densities, namely, 25% and 65%, by using Bolton's empirical expressions (Bolton 1986). The corresponding values of the dilatancy angles ( $\psi$ ) was found to vary from  $2^\circ$  to  $16^\circ$  at different stress levels associated with small scale model tests on anchors.

The sand bed, that is, the soil mass below the anchor plate for this experiment was kept 300 mm thick and its mass density was kept equal to the same as the mass density of the sand placed over the anchor plate. The anchor plate was uplifted by using the pulling device along with tie rod and lowered on the 300 mm thick and bed. Sand was poured by using pluviation technique where constant height of fall of pouring sand was maintained for a particular density. The height of fall against relative density was calibrated before performing any pullout test on the anchor.

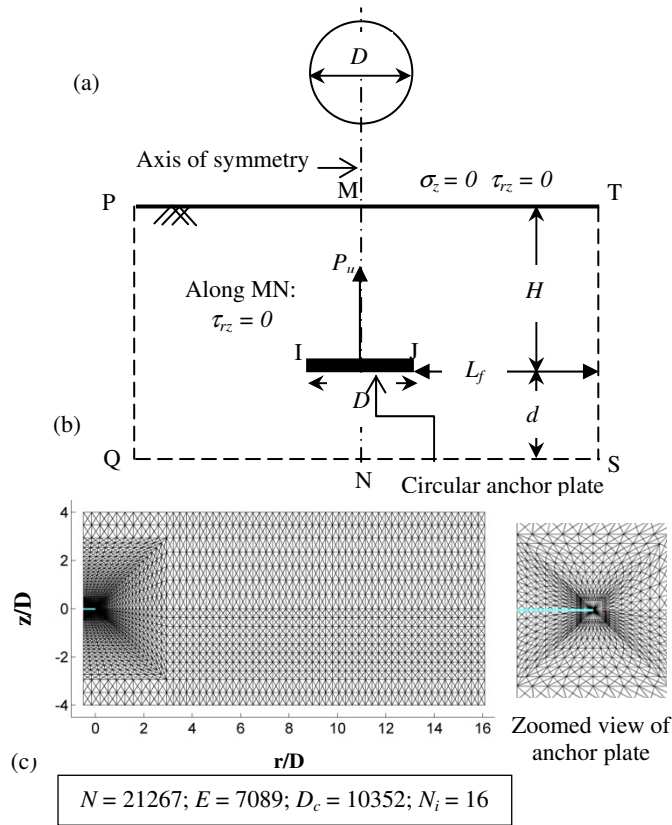


Figure 1 A schematic diagram of the problem with (a) plan view of circular anchor plate; (b) front view of the problem domain with boundary conditions; (c) typical finite element mesh for  $H/B = 4$

The friction angle ( $\phi_{cv}$ ) corresponding to the critical void ratio for the chosen sand was found to be  $31^\circ$ . It is understood that the peak friction angle of sand varies with the stress level (Bolton 1986). The vertical normal stress, as mentioned earlier, while performing direct shear stress tests was kept in a range of 50-150 kPa. This range of the stress level is, however, greater than the average stress level in small scale tests which are performed on

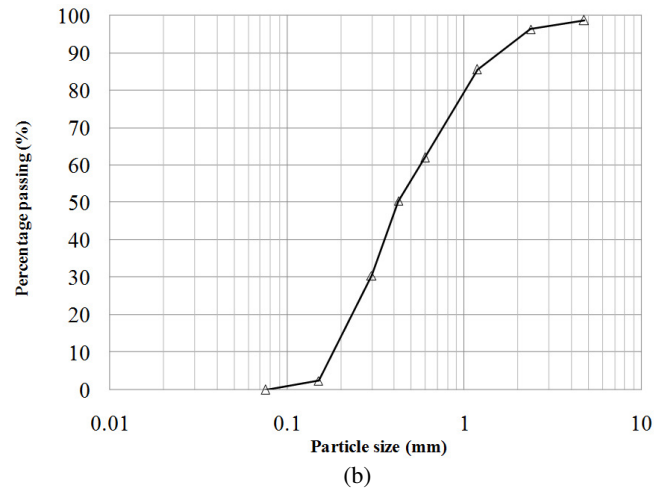
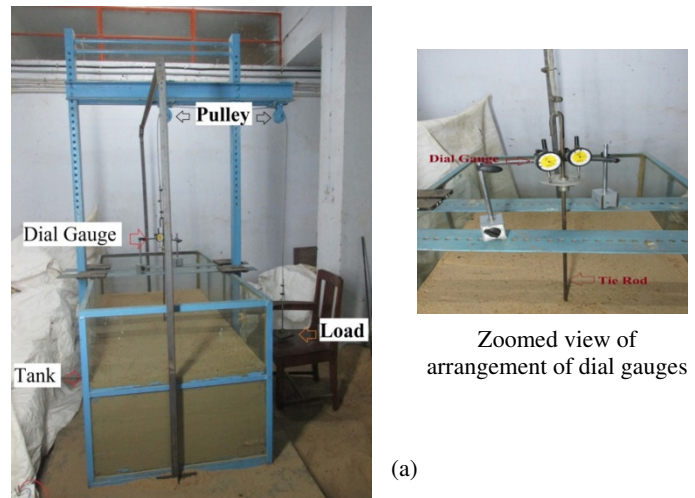


Figure 2 (a) Experimental set up used in laboratory test; (b) Grain size distribution curve of the sand material

5. NUMERICAL MODELLING

A circular anchor plate (IJ) of diameter  $D$  is embedded at a depth  $H$  in homogeneous sand stratum as shown in Figure 1. The anchor plate is subjected to vertical pullout load. Since the entire problem remains symmetric about an axis MN passing through the centre of the circular plate, the planar domain (MNST) in  $r-z$  axes, with the axis of the symmetry as one of the boundary, was chosen for doing the numerical analysis. The soil internal frictional angle ( $\phi$ ) has been

assumed to be constant throughout the soil domain for the numerical studies. The lower and upper bounds solutions bracket the true collapse load from above and below, respectively. The numerical analysis is carried out by using the lower bound limit analysis in conjunction with finite elements. The soil medium is assumed to obey the Mohr-Coulomb failure criterion and an associated flow rule so that the lower bound theorem of the limit analysis remains applicable. In order to carry out the lower bound limit analysis, the vertical boundary (ST) and the horizontal boundary (NS) of the domain need to be kept at sufficient distances away from the anchor plate. The horizontal distance ( $L_f$ ) between the right end of the anchor plate and the vertical boundary ST is varied from  $15D$  to  $25D$  for different values of  $\phi$  and  $H/D$ . On the other hand, the vertical distance between the bottom face of the anchor plate and the horizontal boundary NS is varied between  $3D$  and  $15D$  depending upon the values of  $\phi$  and  $H/D$ . The values of  $L_f$  and  $d$  are selected in a manner such that (i) the yielded elements do not approach towards any of the chosen domain boundaries (ST and NS), and (ii) an increment in the size of the domain, than that chosen, does not bring any change in the magnitude of the collapse load.

The stress boundary conditions that are applicable along the different boundaries of the domain are presented in Figure 1(b). The values of  $\sigma_z$  and  $\tau_{rz}$  are equal to  $q$  and zero, respectively, along the stress free ground surface (MT). No stress boundary conditions need to be specified along the boundaries ST and NS. A shear slip is permitted between the interfaces of the horizontal anchor plate and the surrounding soil mass. Along the anchor-soil interface, both top and bottom, the following stress boundary condition is imposed:

$$|\tau_{rz}| \leq (c \cot \phi - \sigma_z) \tan \delta \quad (3)$$

The negative sign attached with normal stress,  $\sigma_z$ , arises due to the fact that tensile normal stresses are considered as positive in the analysis. The value of  $\delta$  has been taken equal to  $\phi$ .

The problem domain is discretized into a number of three noded triangular elements in a way such that the sizes of the elements reduce continuously towards the edge (singular point) of the anchor plate. A typical finite element mesh, for the embedment ratio ( $H/D$ ) equal to 4, is shown in Figure 1 (c) with  $\phi = 30^\circ$ ; where  $N$ ,  $E$ ,  $D_c$  and  $N_i$  are total number of nodes, elements, stress discontinuities and nodes along the soil-anchor interface on each side of the anchor plate, respectively, present in the statically admissible stress field. The methodology followed in this study was earlier proposed by Kumar and Khatri (2011) where  $\sigma_r$ ,  $\sigma_z$ ,  $\sigma_\theta$  and  $\tau_{rz}$  for a circular anchor, are considered as the basic unknown stress variables. Each element present in the stress field should satisfy the element equilibrium condition. Statically admissible stress discontinuities were permitted by keeping the normal and shear stresses continuous along all the common edges shared by any two adjacent elements. It was also specified that the yield condition does not get violated anywhere in the stress field. The present finite element formulation finally becomes a linear programming problem where the original Mohr-Coulomb yield surface is linearized by a regular polygon of  $p$  sides inscribed to the parent yield surface by following Bottero et al. (1980); the value of  $p$  in the present study was taken equal to 21. The  $p$  numbers of inequality constraints need to be satisfied at each point in the stress field. The value of one additional stress variable,  $\sigma_\theta$ , other than  $\sigma_r$ ,  $\sigma_z$  and  $\tau_{rz}$ , is kept closer to the minor principal stress  $\sigma_3$  following Harr-von Karman hypothesis. Finally the linear programming problem is stated in a standard canonical form:

Maximize the objective function:  $-\{c\}^T \{\sigma\}$  (4)

Subjected to (i) equality constraints:  $[A_{eq}]\{\sigma\} = \{b_{eq}\}$  (5)

(ii) inequality constraints:  $[A_{ineq}]\{\sigma\} \leq \{b_{ineq}\}$  (6)

The linear optimization was accomplished by using LINPROG, an in-build library functions available in MATLAB.

## 6. RESULTS

### 6.1 Laboratory test results

#### 6.1.1 Variation of experimental pullout capacity factors and its comparison with numerical result

The load versus displacement curves of the anchor plates embedded in sands, for two different relative densities, with different embedment ratios ( $H/D = 2, 3, 4, 5$ ) are plotted in Figures 3(a) and 3(b). It is observed from Figures 3(a) and 3(b) that the failure load increases continuously with an increase in the magnitude of the embedment ratio and relative density. The ultimate uplift resistance of the anchor plates for different combinations of relative densities and embedment ratios were determined from Figures 3(a) and 3(b).

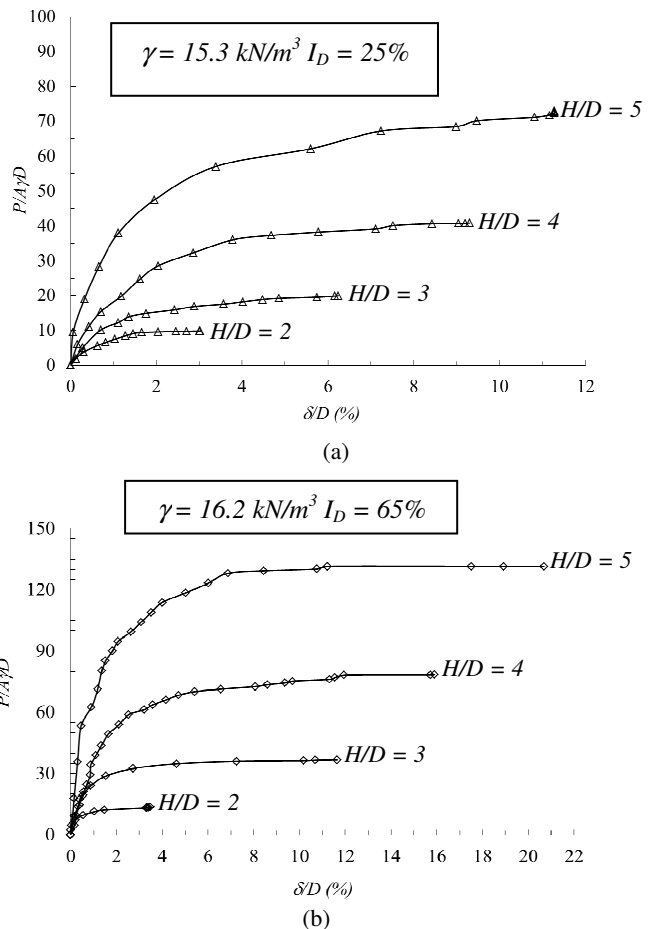


Figure 3 Load-displacement response for: (a) loose sand,  $I_D = 25\%$ , and (b) medium dense sand,  $I_D = 65\%$

Accordingly, the vertical pullout capacity of the circular anchor was evaluated experimentally for different values of embedment ( $H/D$ ) and relative density of sand by using Eq. (1), and is illustrated in Figure 4 for different combinations of  $H/D$  and  $I_D$ . The magnitude of the upward vertical displacement experienced by circular anchor plate at failure is found to increase from  $0.03D$  to  $1.2D$  for different values of  $H/D$  when the anchor plate is embedded in loose sand. On the other hand, the circular anchor plate embedded in a medium dense sand, undergoes, relatively, to a higher magnitude of vertically upward displacement varying from  $0.035D$  to  $2.2D$  for different embedment ratios. It is also observed from the variation of the pullout capacity factor ( $F_\gamma$ ) versus embedment depth ( $H$ ) plots that the pullout capacity increases continuously with an increase in the embedment depth ( $H$ ).

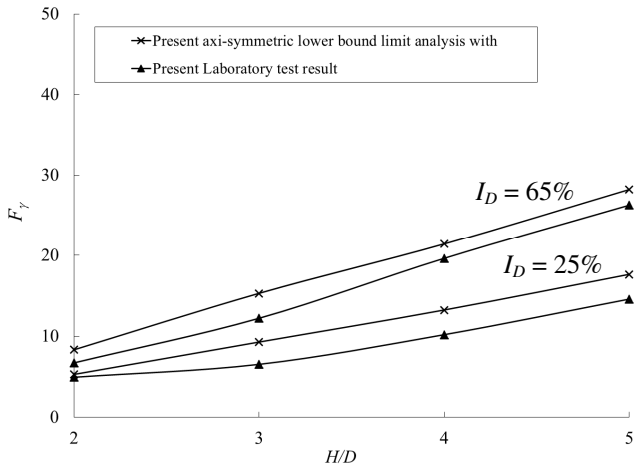


Figure 4 A comparison of obtained values of experimental and theoretical pull out factors

The numerical values of  $F_\gamma$  given in Figure 4 are based on non-associated flow rules with dilatancy angle varying between  $2^\circ$  and  $16^\circ$ . The effect of the stress level has also been incorporated while making the comparison; the magnitude of  $\phi_p$  was determined corresponding to an average normal stress of  $p_v/2$ . Limit theorems are strictly applicable for an associated flow rule. However, one can approximately find out the magnitude of the collapse load for a sand following a non-associated flow rule (Sloan, 2013) by using the reduced internal frictional  $\phi^*$ , instead of  $\phi$ , based on the expressions given by Davis (1968):

$$\tan \phi^* = \eta \tan \phi, \text{ and } \eta = \frac{\cos \psi \cos \phi}{1 - \sin \psi \sin \phi} \quad (7)$$

By making use of  $\phi^*$ , the magnitude of the collapse load can be accordingly obtained for any a given value of dilatancy angle ( $\psi$ ).

It can be noted from Figure 4 that the pullout capacity factors obtained from the experimental investigation for loose to medium sands at two different relative densities have been found to marginally smaller than the present numerical solution obtained by using the axisymmetric lower bound finite element analysis. This difference is expected due to progressive shear failure effect in experiments, that is, the peak states (for finding peak internal friction angles) of sand do not occur simultaneously in the domain.

**6.1.2 The variation of maximum settlement of anchor plate at failure**

The variation of the settlements at failure in non-dimensional form ( $\delta_f/D$ ) with embedment ratios has been studied in Figure 5(a). It has been observed in Figure 5(a) that the anchor plate experiences greater settlements before failure with an increase (i) in the relative density from loose to medium dense sand, and (ii) in the embedment ratio of the anchor plate.

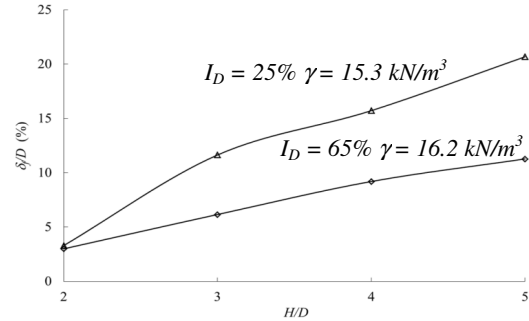
**6.1.3 The variation of the initial stiffness**

The variation of the initial stiffness, which is defined in a non-dimensional form ( $K_i = \frac{d(F_\gamma/L\gamma D)}{d(H/D)}$ ), is plotted in Figure 5(b). It is noticed that the initial stiffness becomes a function of the embedment ratio and the relative density of sand. The initial stiffness increases with an increase in the values of embedment ratio and relative density of sand.

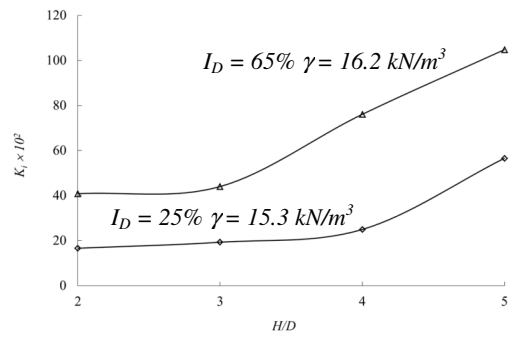
**6.2 Numerical results**

**6.2.1 The variation of the pullout capacity factors**

The variation of the pullout capacity factors ( $F_\gamma$  and  $F_q$ ) with changes in embedment ratio of the circular anchor plate for different values of soil frictional angle ( $\phi$ ) as obtained from the numerical analysis is shown in Figures 6(a) and 6(b). The two pullout capacity factors,  $F_\gamma$  and  $F_q$ , have been found to increase continuously with an increase in the embedment ratio of anchor plate and the internal friction angle of soil mass.

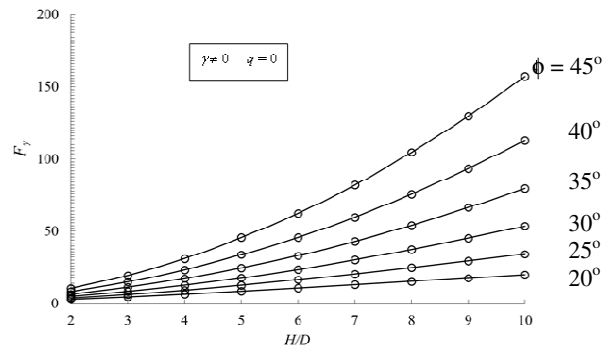


(a)

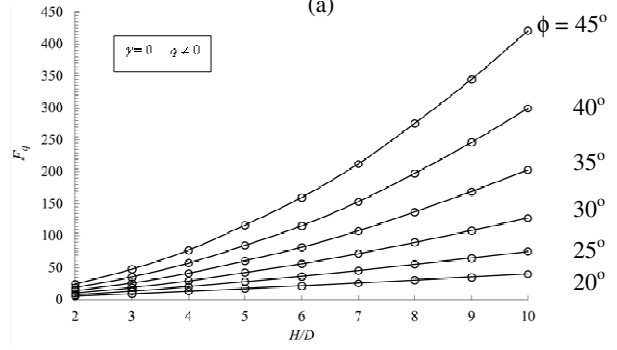


(b)

Figure 5 The variation of (a)  $\delta_f/D$  with  $H/D$  for different values of  $\phi$ , (b) the initial stiffness ( $K_i$ ) with  $H/D$  for different values of  $\phi$



(a)



(b)

Figure 6 The variation of (a)  $F_\gamma$  with  $H/D$  and  $\phi$ , and (b)  $F_q$  with  $H/D$  and  $\phi$

**6.2.2 Comparison of the pullout capacity factors with the available data from literature**

The values of the pullout capacity factor  $F_\gamma$  obtained from the numerical analysis were compared with the available numerical and experimental results from literature. The comparisons are shown in Figures 7(a) and 7(b). The present numerical results are found to be 5~10% higher than the solutions provided by Merifield et al. (2006) on the basis of the three dimensional lower bound limit analysis. It can also be noted that the present solution is about 10~30% higher than the solution provided by Murray and Geddes (1987) by using the limit equilibrium method for  $\phi = 40^\circ$  but it becomes 2~5% lesser for  $\phi = 30^\circ$ . In the limit equilibrium method, a failure surface is assumed and an assumption of the stress distribution was also made along the failure surface. No such assumption is, however, sought in the present numerical limit analysis. The trends of the present results match well with the solution provided by Koutsabeloulis and Griffiths (1989) for the trapdoor problems by using the finite element method on the basis of the non-associated flow rule.

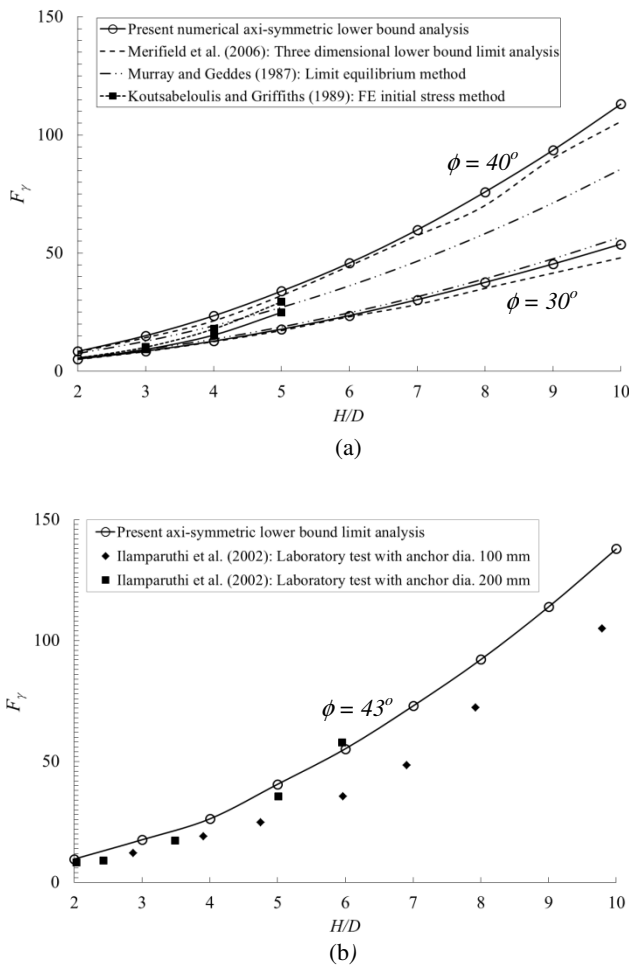


Figure 7 A comparison of present results from the numerical analysis with the data available from literature by (a) different analyses and (b) experimental investigations

Note that the present numerical results always provide slightly greater values of the pullout factors as compared to the solutions provided by Koutsabeloulis and Griffiths (1989). The present numerical results match well with the experimental results given by Ilamparuthi et al. (2002) for circular anchor plates having two different diameters, namely, 100 mm and 200 mm.

**6.4 Proximity of the stress state to yield**

After finding out the statically admissible stress field, the proximity of the stress state to yield has been found out by calculating the  $a/d$  ratio, where  $a = (\sigma_r - \sigma_z)^2 + (2\tau_{rz})^2$  and  $d = (\sigma_r + \sigma_z)^2 \sin^2 \phi$ . The variation of  $a/d$  ratio in the problem domain has been presented in Figures 8(a) and 8(b) corresponding to the value of  $H/D$  equal to 3 and 5 with  $\phi = 40^\circ$ . It is noticed that for  $H/D = 3$ , the failure zone starts from the edge of the anchor plate and it approaches towards the ground surface. However, for  $H/D = 5$ , the failure zone does not reach to the ground surface. Note that the size of the plastic zone increases with an increase in the value of the embedment ratio.

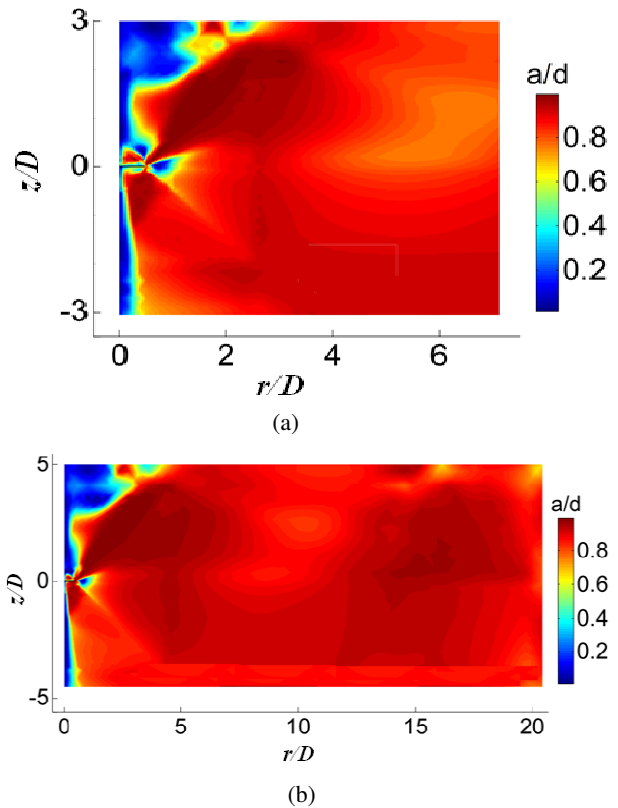


Figure 8 The proximity of the stress state to the yield for medium dense sand ( $\phi = 40^\circ$ ) for (a)  $H/B = 3$  and (b)  $H/B = 5$

**7. CONCLUSIONS**

The present work presents experimental and numerical investigations on finding out the vertical uplift resistance of circular plate anchors embedded in a sand stratum for a wide range of embedment ratios. The numerical investigation is based on the lower bound theorem of the limit analysis in combination with finite elements and linear programming for a range of  $H/D$  varying from 2 to 10. On the other hand, experimental model tests are restricted for the value of  $H/D$  varying from 2 to 5. It has been noted that the pullout capacity factors increase continuously with an increase in the embedment ratio as well as the internal friction angle of sand. The magnitudes of the displacement to cause the ultimate failure and the initial stiffness of the load versus deformation plots have been found to increase continuously with an increase in the embedment ratio and the relative density of sand. The failure pattern plots from the numerical analysis reveal that the plastic zone reaches up to ground surface for shallow anchors. On the other hand, for deep anchors, the development of the failure surface is restricted only up to a certain limited depth above the anchor plate.

## 8. REFERENCES

- Baker, W. H., and Konder, R. L. (1966) "Pullout load capacity of a circular earth anchor buried in sand", *Highway Res. Rec.*, 108, pp1-10.
- Balla, A. (1961) "The resistance of breaking-out of mushroom foundations for pylon", *Proceedings of 5<sup>th</sup> International Conference on Soil Mechanics and Foundation Engineering*, Paris, 1, pp 569-576.
- Bolton, M. D. (1986) "The strength and dilatancy of sands", *Geotechnique*, 36, Issue 1, pp 65–78.
- Bottero, A., Negre, R., Pastor, J., and Turgeman, S. (1980) "Finite element method and limit analysis theory for soil mechanics problem", *Computer Methods in Applied Mechanics and Engineering*, 22, Issue 1, pp 131-149.
- Das, B. M., and Seeley, G. R. (1975) "Breakout Resistance of shallow horizontal anchors", *Journal of Geotechnical Engineering, Division, ASCE*, 101, Issue 9, pp 999-1003.
- Davis, E. H. (1968) "Theories of plasticity and failure of soil masses in *Soil Mechanics: selected topics*", edition. I. K. Lee, pp 341-354, New York, USA, Elsevier.
- Dickin, E. A. (1988) "Uplift behavior of horizontal anchor plates in sand", *Journal of Geotechnical Engineering, ASCE*, 114, Issue 11, pp1300-1317.
- Ilamparuthi, K., Dickin, E. A., and Muthukrisnaiah, K. (2002) "Experimental investigation of the uplift behaviour of the circular plate anchors embedded in sand", *Canadian Geotechnical Journal*, 39, Issue 3, pp 648-664.
- Indian Standard Code (IS 2720 Part 4). (1985, Reaffirmed 1997) *Method of Test for Soils - Part 4 Direct Shear Test*, 2<sup>nd</sup> revision, pp 5-11.
- Indian Standard Code (IS 2720 Part 13). (1986, Reaffirmed 1995) *Method of Test for Soils - Part 4 Grain Size Analysis*, 2<sup>nd</sup> revision, pp 4-8.
- Khatri, V. N., and Kumar, J. (2011) "Effect of anchor width on pullout capacity of strip anchors in sand", *Canadian Geotechnical Journal*, 48, Issue 3, pp 511-517.
- Koutsabeloulis, N. C. and Griffiths, D. V. (1989) "Numerical modelling of the trapdoor problem", *Geotechnique*, 39, Issue 1, pp77–89.
- Kumar, J. (2001) "Seismic vertical uplift capacity of strip anchors", *Geotechnique*, 52, Issue 2, pp 79-88.
- Kumar, J., and Khatri, V. N. (2011) "Bearing capacity factors of circular foundations for a general  $c-\phi$  soil using static finite element analysis", *International Journal of Numerical and Analytical Methods in Geomechanics*, 35, Issue 3, pp 393-405.
- Kumar, J., and Kouzer, K. M. (2008) "Vertical uplift capacity of horizontal anchors using upper bound limit analysis and finite elements", *Canadian Geotechnical Journal*, 45, Issue 5, pp 698-704.
- Merifield, R. S., Lyamin A. V., and Sloan, S. W. (2006) "Three dimensional lower bound solutions for the stability of plate anchors in sand", *Geotechnique*, 56, Issue 2, pp 123–132.
- Merifield, R. S., and Sloan, S. W. (2006) "The ultimate pullout capacity of anchors in frictional soils", *Canadian Geotechnical Journal*, 43, Issue 8, pp 852-868.
- Meyerhof, G. G. (1973) "Uplift resistance of inclined anchors and piles", *Proceedings of 8<sup>th</sup> International Conference on Soil Mechanics and Foundation Engineering*, Moscow, 2, pp 167-172.
- Murray, E. J., and Geddes, J. D. (1987) "Uplift of anchor plates in sand", *Journal of Geotechnical Engineering, ASCE*, 113, Issue 3, pp 202-215.
- Rowe, R. K., and Davis, E. H. (1982) "The behaviour of anchor plates in sand", *Geotechnique*, 32, Issue 1, pp 25-41.
- Sloan, S. W. (2013) "Geotechnical stability analysis", *Geotechnique*, 63, Issue 7, pp531-572. Rankine Lecture.
- Sutherland, H. B. (1965) "Model studies for shaft raising through cohesionless soil", *Proceedings of 3<sup>rd</sup> International Conference on Soil Mechanics and Foundation Engineering*, Montreal, Canada, 2, pp 410-413.